

20 **Abstract:**

21 Reactive sulfane sulfur species such as hydrogen polysulfide and organic persulfide
22 are newly recognized as normal cellular components, involved in signaling and
23 protecting cells from oxidative stress. Their production is extensively studied, but
24 their removal is less characterized. Herein, we showed that reactive sulfane sulfur is
25 toxic at high levels, and it is mainly removed via reduction by thioredoxin and
26 glutaredoxin with the release of H₂S in *Escherichia coli*. OxyR is best known to
27 respond to H₂O₂, and it also played an important role in responding to reactive sulfane
28 sulfur under both aerobic and anaerobic conditions. It was modified by hydrogen
29 polysulfide to OxyR C199-SSH, which activated the expression of thioredoxin 2 and
30 glutaredoxin 1. This is a new type of OxyR modification. Bioinformatics analysis
31 showed that OxyRs are widely present in bacteria, including strict anaerobic bacteria.
32 Thus, the OxyR sensing of reactive sulfane sulfur may represent a conserved
33 mechanism for bacteria to deal with sulfane sulfur stress.

34

35 **Keywords:** OxyR, reactive sulfane sulfur, oxidative stress, *Escherichia coli*,
36 thioredoxin, glutaredoxin

37

38 **Introduction:**

39 H₂S has been proposed as a gasotransmitter because it is involved in many
40 physiological and pathological processes in animals and plants, such as ageing (*Hine*
41 *et al*, 2015), neuromodulation (*Abe & Kimura, 1996*), cancer cell proliferation (*Cai et*
42 *al*, 2010), metabolic reprogramming (*Gao et al*, 2015), and stomatal closure in plant
43 (*Lisjak et al*, 2010). The mechanism of H₂S signaling is often via protein
44 persulfidation or S-sulfhydration. Since H₂S cannot direct react with protein thiols, its
45 oxidation product reactive sulfane sulfur, which can readily react with thiols to
46 generate persulfides, has been identified (*Mishanina et al*, 2015; *Toohey*, 2011).
47 Reactive sulfane sulfur species include hydrogen polysulfides (H₂S_n, n≥2), organic
48 polysulfides (RSS_nH, RSS_nR, n≥2), and organic persulfides (RSSH), which can also
49 be produced directly from cysteine or cystine, and they are now considered as normal
50 components in both prokaryotic and eukaryotic cells (*Sawa et al*, 2018; *Yadav et al*,
51 2016). They possess both nucleophilic and electrophilic characteristics, while thiols
52 (cysteine, GSH, etc.) are generally nucleophilic (*Ono et al*, 2014; *Park et al*, 2015).
53 As nucleophiles, they are better reductants than thiols (*Ida et al*, 2014); as
54 electrophiles, the electrophilic sulfane sulfur (S⁰) can be transferred to protein thiols
55 to generate protein-SSH, which modifies enzyme activities and protects proteins from
56 irreversible oxidation (*Mustafa et al*, 2009; *Paul & Snyder*, 2015). Owing to these
57 unique dual-reactivities, reactive sulfane sulfur is involved in many cellular processes,
58 such as redox homeostasis maintenance, virulence regulation in pathogenic bacteria,
59 and biogenesis of mitochondria (*Fujii et al*, 2018; *Peng et al*, 2017). Albeit the good

60 roles, sulfane sulfur may be toxic at high concentrations. Indeed, elemental sulfur has
61 been used as an antimicrobial agent for ages, and its efficiency is likely impaired by
62 its low solubility (*Williams & Cooper, 2010*). Due to its low solubility, elemental
63 sulfur is not considered as a reactive sulfane sulfur species. Advances in the synthesis
64 of sulfur nanoparticles have significantly increased the antimicrobial efficiency of
65 sulfur (*Rai et al, 2016*). Sulfur is often used as a fungicide. Although its toxicity
66 mechanism is unclear, a recent study suggested that sulfur is transported into the cell
67 in the form of hydrogen polysulfide (*Sato et al, 2011*), inducing protein persulfidation
68 as a possible toxic mechanism (*Islamov et al, 2018*). Fungi may use glutathione to
69 reduce polysulfides to H₂S as a detoxification mechanism (*Samrat et al, 2013; Sato et*
70 *al, 2011*). Organosulfur compounds can be used to treat antibiotic-resistant bacteria,
71 and they are converted to hydrogen polysulfide inside the cells for the toxicity (*Xu et*
72 *al, 2018*). Both bacteria and fungi show reduced viability being exposed to sulfane
73 sulfur stress (*Sato et al, 2011; Xu et al, 2018*). Therefore, intracellular sulfane sulfur is
74 likely maintained within a range for microorganisms under normal conditions.

75 Multiple pathways for sulfane sulfur generation have been discovered.
76 Cystathionine β-synthase and cystathionine γ-lyase produce sulfane sulfur from
77 cystine (*Ida et al, 2014*); 3-mercaptopyruvate sulfurtransferase (3-MST) and
78 cysteinyl-tRNA synthetase (CARS) produce sulfane sulfur from cysteine (*Akaike et al,*
79 *2017; Nagahara et al, 2018*); Sulfide:quinone oxidoreductase and superoxide
80 dismutase (SOD) produce sulfane sulfur from H₂S (*Olson et al, 2018; Xin et al, 2016*).
81 Catalase can oxidize H₂S and polysulfides to sulfur oxides (*Olson et al, 2017*). Most

82 microorganisms possess several of these pathways. On the flipside, elimination
83 pathways are less investigated. Aerobic microorganisms may apply persulfide
84 dioxygenase to remove excessive sulfane sulfur (*Xia et al, 2017*), and the persulfide
85 dioxygenase expression can be induced by sulfane sulfur via sulfane sulfur-sensing
86 transcription factors (*H et al, 2017; Lira et al, 2018; Luebke et al, 2014*).

87 For anaerobic microorganisms that dominate in the intestinal tract, their sulfane
88 sulfur elimination pathways are ambiguous. A reasonable hypothesis is that they use
89 glutathione (GSH) or NADPH to reduce sulfane sulfur to H₂S and then release it out
90 of cells (*Carbonero et al, 2012*), as observed in anaerobically cultured fungi (*Abe et al,*
91 *2007; Sato et al, 2011*). A recent report that two thioredoxin-like proteins catalyze the
92 reduction of protein persulfidation in *Staphylococcus aureus* also support the
93 hypothesis (*Peng et al, 2017*). However, it is unclear whether sulfane sulfur induces
94 the expression of these enzymes.

95 *Escherichia coli*, a common intestinal bacterium, contains three thioredoxins and
96 four glutaredoxins. The expression of TrxA, GrxB, and GrxD is regulated by
97 guanosine 3',5'-tetrphosphate, and the expression of GrxC is regulated by cAMP,
98 both of which are nutrient related messengers (*Lim et al, 2000; Srivatsan & Wang,*
99 *2008*). These four enzymes are highly abundant in *E. coli*; together they account for
100 more than 1% of total protein (*Fernandes et al, 2005; Fernandes & Holmgren, 2004;*
101 *Ritz et al, 2000*). The expression of GrxA, TrxC, and KatG (catalase) is regulated by
102 OxyR upon exposure to H₂O₂. Without oxidative stress, these proteins are much lower
103 than other thioredoxins and glutaredoxins (*Fernandes & Holmgren, 2004;*

104 *Gutierrez-Ríos et al, 2007; Ritz et al, 2000).*

105 OxyR was initially identified as a regulator responding to reactive oxygen
106 species (ROS) (*Christman et al, 1985; Storz et al, 1990*). ROS triggers the formation
107 of intra disulfide bond between Cys¹⁹⁹ and Cys²⁰⁸ or oxidizes Cys¹⁹⁹ to C199-SOH.
108 The exact mechanism is still in debate (*Choi et al, 2001; Kim et al, 2002; Zheng et al,*
109 *1998*). Three additional modifications on Cys199 (C199-SNO, C199-SSG and
110 avicinylation) are also known, which result in different OxyR configurations, DNA
111 binding affinities, and promoter activities (*Haridas et al, 2005; Kim et al, 2002; Seth*
112 *& Stamler, 2012*). Thus, OxyR leads to multi-levels of transcriptional responses when
113 responding to different stress signals.

114 Herein, we systematically investigated the sulfane sulfur reduction activity and
115 expression pattern of thioredoxins, glutaredoxins, and KatG in *E. coli*. We found that
116 these enzymes are responsible for maintaining the homeostasis of intracellular sulfane
117 sulfur. Further investigation unveiled a new and H₂S_n-specific modification of OxyR.

118

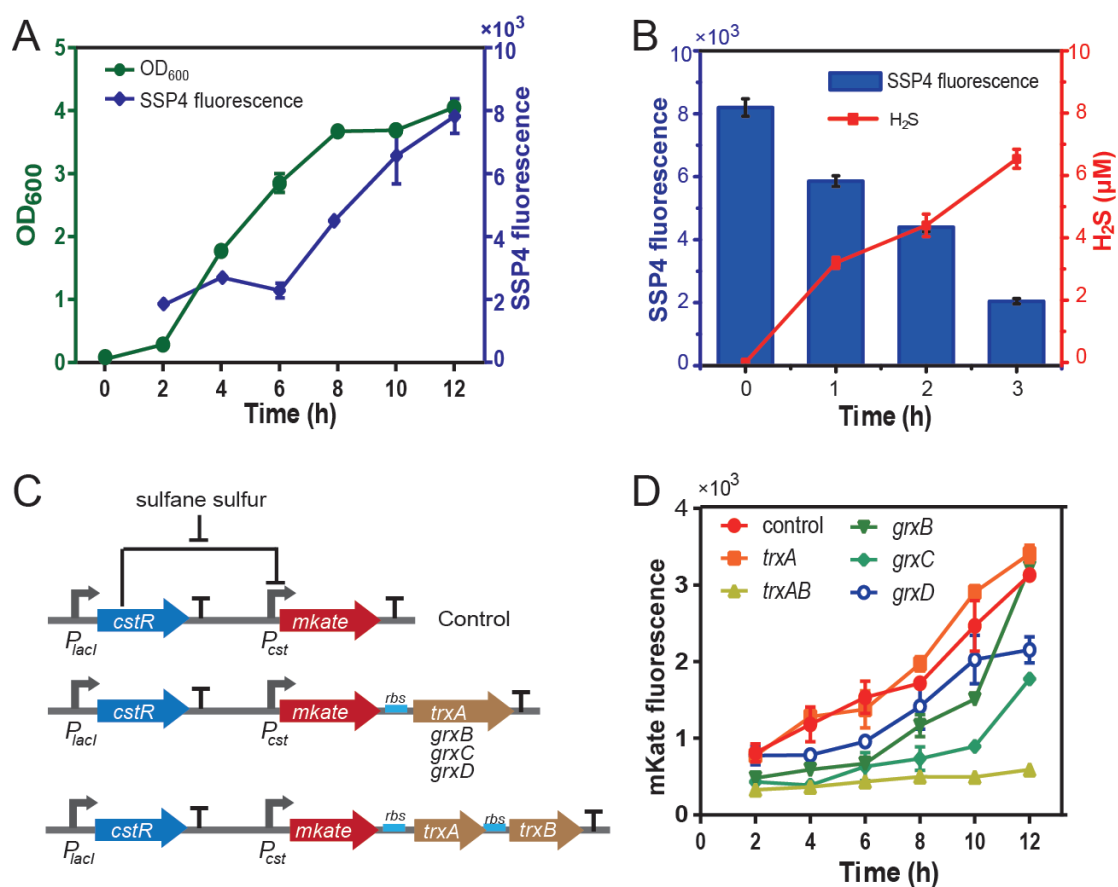
119 **Results:**

120 *The accumulation and reduction of endogenous sulfane sulfur in E. coli*

121 *E. coli* has endogenous sulfane sulfur producing enzymes, including CARS,
122 3-MST, SodA, and SodC (*Akaike et al, 2017; Nagahara et al, 2018; Olson et al,*
123 *2018*). We cultured early-log phased *E. coli* cells in LB medium and used the sulfane
124 sulfur sensitive probe SSP4 (Fig. 1A) to detect intracellular sulfane sulfur. The
125 intracellular sulfane sulfur started to accumulate at middle-log phase and reached the

126 maximum at early stationary phase. On the other hand, when the stationary-phased
 127 cells were transferred into fresh medium ($OD_{600}=1$), their intracellular sulfane sulfur
 128 decreased quickly with concomitant release of H_2S (Fig. 1B). This phenomenon
 129 suggests that sulfane sulfur may be reduced to H_2S by enzymes, such as thioredoxin
 130 and glutaredoxin (Dóka et al, 2016; Wedmann et al, 2016).

131



132

133 **Fig. 1. Endogenous sulfane sulfur production and reduction in *E. coli*.** A) *E. coli* accumulated
 134 sulfane sulfur and released H_2S during late-log and stationary phases. B) Stationary-phased *E. coli*
 135 reduced intracellular sulfane sulfur to H_2S after being transferred to fresh LB. C) CstR-based reporters
 136 for real-timely monitoring intracellular sulfane sulfur. D) Overexpression of thioredoxins and
 137 glutaredoxins decreases intracellular sulfane sulfur, as indicated by mKate fluorescence.

138

139 *Thioredoxin and glutaredoxin participate in the reduction of intracellular sulfane*

140 *sulfur*

141 To confirm the change of intracellular sulfane sulfur *in vivo*, we constructed a
142 transcription factor (TF)-based reporting plasmid, which contained a sulfane
143 sulfur-sensing TF (CstR) (*Luebke et al, 2014*), its cognate promoter (*Pcst*), and a red
144 fluorescent protein (mKate, with a C-terminus degradation tag *ssrA*) (Fig. 1C). Using
145 the reporting plasmid, the increase of intracellular sulfane sulfur in live cells (Fig. 1A)
146 was reported as the mKate fluorescence (Fig. 1D). When GrxB, GrxC, or GrxD was
147 co-transcribed with mKate under the control of CstR, their expression could partially
148 decrease the sulfane sulfur accumulation as reflected with the mKate fluorescence
149 intensity (Fig. 1D). When TrxA was co-transcribed, it did not affect sulfane sulfur
150 accumulation (Fig. 1D). However, when thioredoxin reductase (TrxB) was
151 co-expressed with TrxA, sulfane sulfur were not increased during the log phase of
152 growth (Fig. 1D). These results indicate that thioredoxin and glutaredoxin reduce
153 sulfane sulfur inside *E. coli*.

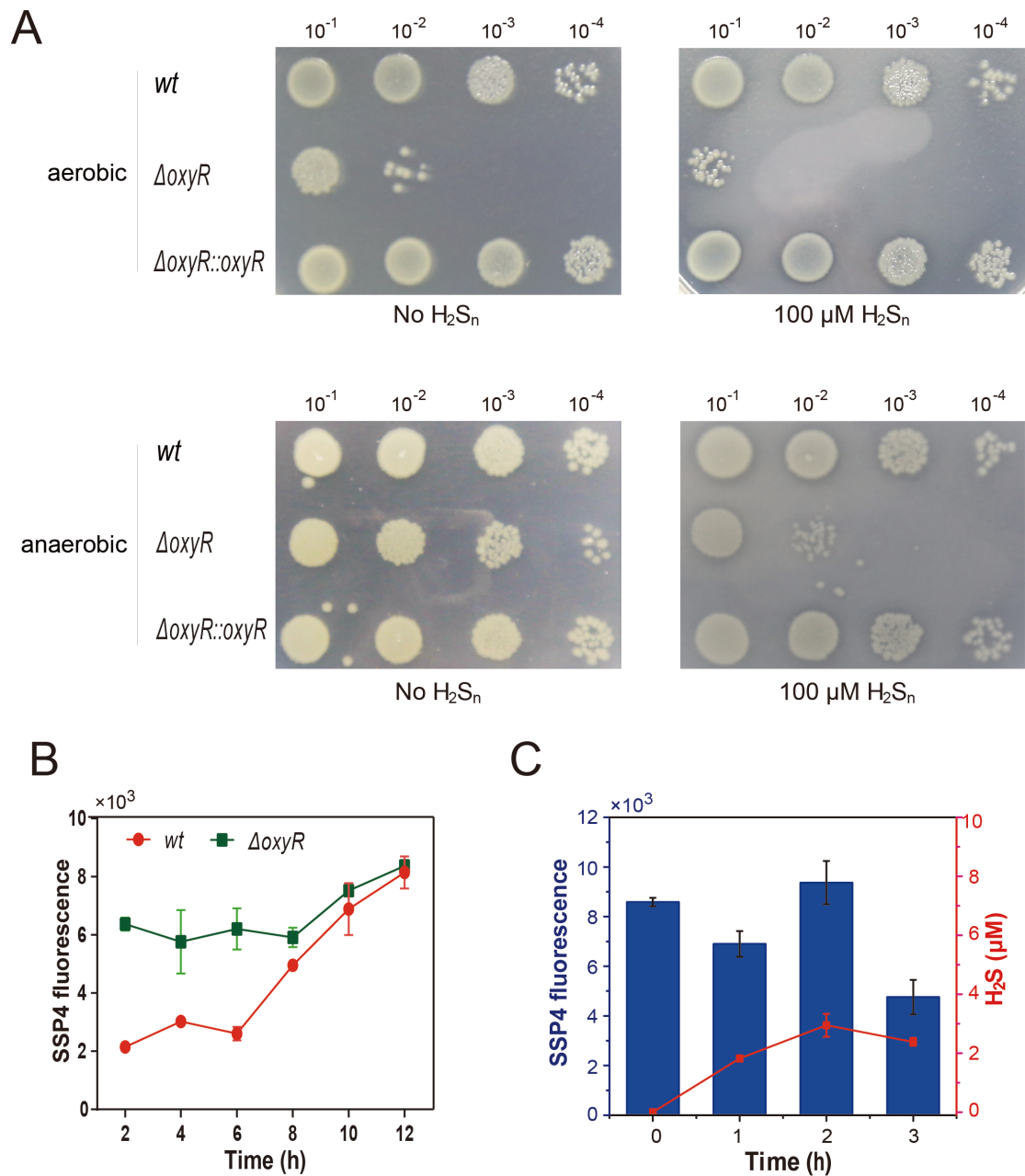
154 The artificial operons contained a negative feedback loop when coupled with an
155 enzyme that reduces sulfane sulfur (Fig. 1C&D). The loop effectively maintained
156 intracellular sulfane sulfur levels within a narrow range, defined by the leaky strength
157 of *Pcst* and the sensitivity of CstR as well as the controlled enzyme activity. Since
158 OxyR is known to regulate similar enzymes, such as TrxC, GrxA, and KatG, we
159 speculated that OxyR may play a role similar as CstR in the artificial operons (Fig.
160 1C).

161

162 *OxyR alleviates sulfane sulfur stress by regulating the expression of TrxC, GrxA, and*

163 *KatG under both aerobic and anaerobic conditions*

164 We deleted *oxyR* gene in *E. coli* and observed that the mutant became more
165 sensitive to exogenously added H₂S_n under both aerobic or anaerobic conditions (Fig.
166 2A). After complementing *oxyR* into $\Delta oxyR$, the strain reassumed the tolerance to
167 H₂S_n to the same level of the wild type (*wt*) (Fig. 2A). The results indicated that OxyR
168 play an important role in dealing with the exogenously sulfane sulfur stress both
169 under aerobic or anaerobic conditions. Compared with *wt*, $\Delta oxyR$ had higher
170 intracellular sulfane sulfur at log-phase (Fig. 2B). In addition, when the $\Delta oxyR$ cells at
171 the stationary phase were transferred into fresh LB medium at OD₆₀₀ of 1, the
172 decrease of the intracellular sulfane sulfur and release of H₂S were slower than that of
173 the *wt* cells (Fig. 2C and Fig. 1B). The results suggested that OxyR responds to
174 sulfane sulfur and activates the expression of sulfane sulfur reduction enzymes.
175



176

177 **Fig. 2. OxyR affects RSS reduction in *E. coli*.** A) *E. coli* $\Delta oxyR$ is more sensitive to exogenous H_2S_n
 178 stress. B) *E. coli* $\Delta oxyR$ accumulates more endogenous sulfane sulfur than *E. coli* *wt* during growth in
 179 LB. C) Stationary-phased *E. coli* $\Delta oxyR$ reduces endogenous sulfane sulfur to H_2S more slowly than *E.*
 180 *coli* *wt* (Fig. 1B) after being transferred to fresh LB.

181

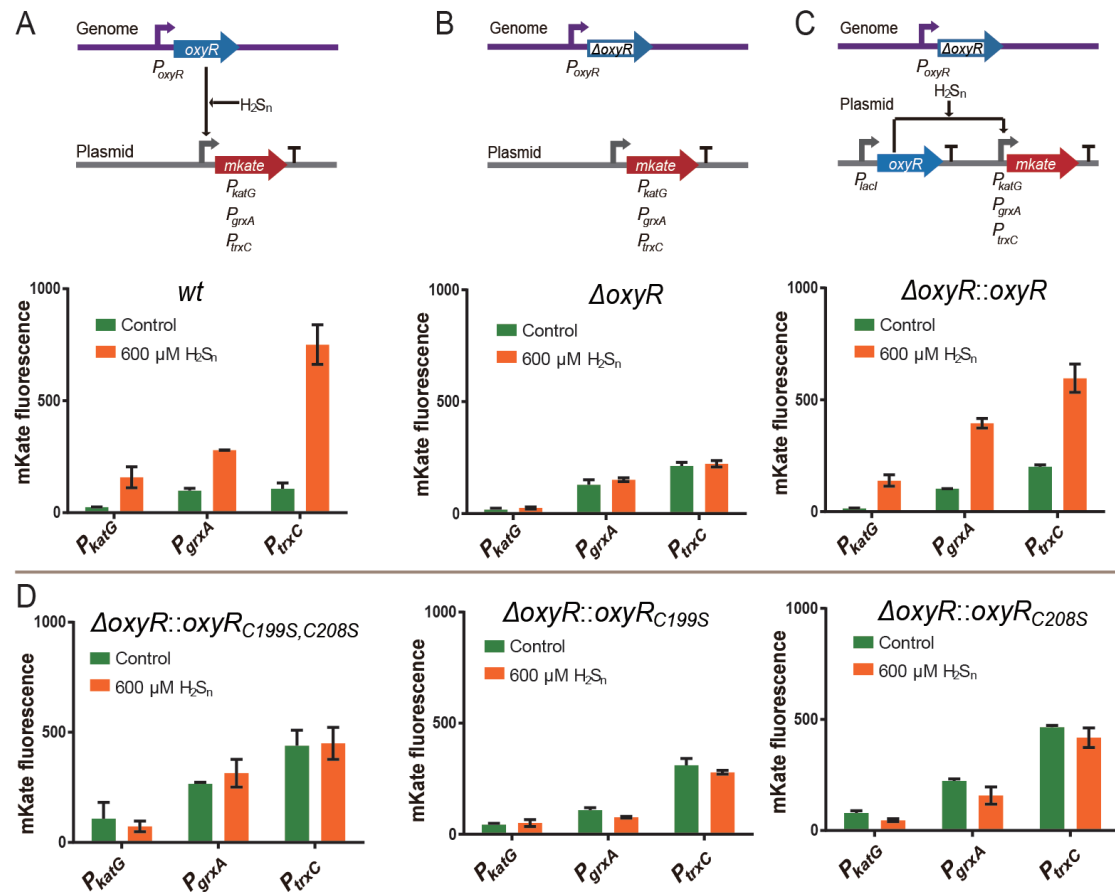
182 To confirm OxyR responds to H_2S_n and activates the expression of *trxC*, *grxA*

183 and *katG*, we constructed three reporting plasmids with an *mKate* gene under the

184 control of a *trxC*, *grxA*, or *katG* promoter. These plasmids were transformed into *E.*

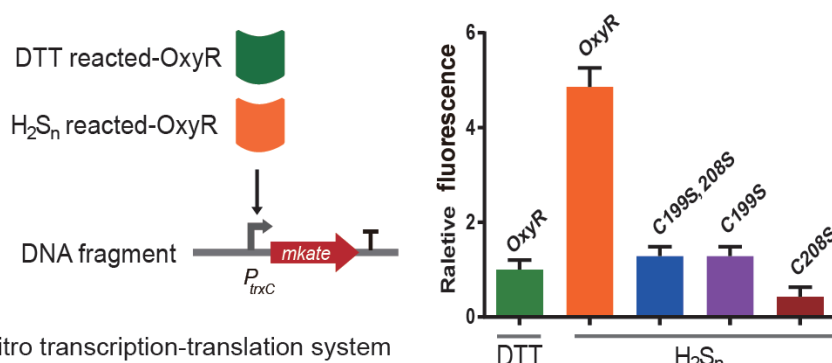
185 *coli* *wt* and $\Delta oxyR$. The recombinant cells were subjected to H_2S_n stress under aerobic

186 conditions. In *wt*, all three promoters led to a low *mKate* expression in the absence of
187 H₂S_n but resulted in obviously higher expression when H₂S_n was added (Fig. 3A).
188 Whereas in the $\Delta oxyR$ strain, the three promoters led to constantly low expression of
189 *mKate* with or without H₂S_n stress (Fig. 3B). After introducing *oxyR* back to $\Delta oxyR$,
190 the promoters performed the same as that in *wt* (Fig. 3C). Further, overexpression of
191 *trxC*, *grxA*, and *katG* in *E. coli* $\Delta oxyR$ decreases intracellular sulfane sulfur (Fig. S1).
192 The induction by H₂S_n was further conformed by *in vitro* transcription-translation
193 experiments. DTT or H₂S_n treated-OxyR and a DNA fragment containing the *trxC*
194 promoter and *mKate* (*P_{trxC}-mKate*) were added into the cell-free
195 transcription-translation system. When DTT-treated OxyR (the reduced form) was
196 used, *mKate* expression was low. Whereas, when H₂S_n-treated OxyR was used, *mKate*
197 expression was significantly increased (Fig. 4). These results indicated that H₂S_n
198 induces the *trxC* promoter via directly modifying OxyR.
199



200
201
202
203
204
205
206

Fig. 3. H_2S_n upregulates expression of *katG*, *grxA*, and *trxC* via OxyR under aerobic conditions. A) H_2S_n induces expression of *katG*, *grxA*, and *trxC* in *E. coli wt*. B) The induction effect is lost in *E. coli* $\Delta oxyR$. C) OxyR complementation recovers the induction effect. D) Cys199 and Cys208 single or double mutants lost the induction effect.



207
208
209

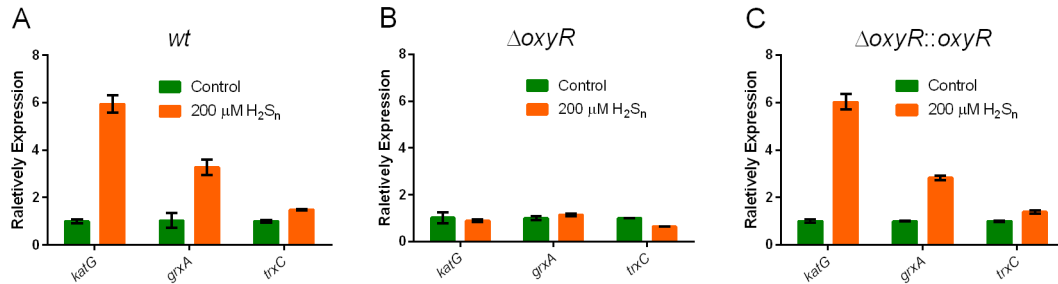
Fig. 4. *In vitro* transcription-translation analysis of H_2S_n activation of OxyR and its mutants.

210
211
212

We also test the induction by H_2S_n under anoxic conditions using qPCR as mKate does not mature under anaerobic conditions. Similarly, *katG*, *grxA*, and *trxC* had higher expression in *wt* when 200 μ M H_2S_n were added (Fig. 5A), but not in

213 $\Delta oxyR$ (Fig. 5B). After complementing $oxyR$ to $\Delta oxyR$, the induction was resumed
214 (Fig. 5C).

215



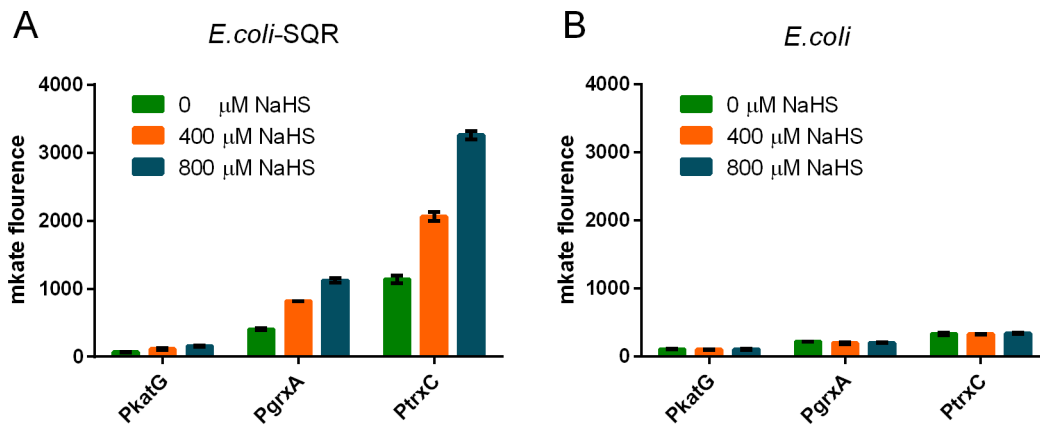
216

217 **Fig. 5. H₂S_n upregulates expression of *katG*, *grxA*, and *trxC* via OxyR under anoxic conditions.** A)
218 H₂S_n induces expression of *katG*, *grxA*, and *trxC* in *E. coli wt*. B) The induction effect is lost in *E. coli*
219 $\Delta oxyR$. C) OxyR complementation recovers the induction effect.

220

221 Since the H₂S_n solution contained some sulfide, we tested if sulfide could induce
222 the gene expression. Sulfide did not induce the expression of related genes in *wt* (Fig.
223 6B), excluding the signal function of sulfide. When we used *E. coli* cells harboring a
224 sulfide:quinone oxidoreductase (SQR) of *C. pinatubonensis* JMP134, the added
225 sulfide was oxidized to H₂S_n (Xin *et al*, 2016), which induced the expression of *trxC*,
226 *grxA* and *katG* (Fig. 6A).

227



228

229 **Fig. 6. The induction of *trxC*, *grxA* and *katG* by NaHS with (A) or without (B) SQR.** The *sqr* of *C.*
230 *pinatubonensis* JMP134 gene was expressed under the *P_{lacI}* promoter in the pBBRmCS2 plasmid.

231

232 *The molecular mechanism of OxyR sensing H₂S_n*

233 OxyR contains six cysteine residues. Previous studies indicated two of them

234 (Cys¹⁹⁹ and Cys²⁰⁸) are involved in ROS sensing (Zheng *et al*, 1998). We constructed

235 an OxyR_{4C→A} mutant (except for Cys¹⁹⁹ and Cys²⁰⁸, the other four cysteines were

236 mutated to alanines) and expressed it in Δ *oxyR*. The mutant regulated *trxC*, *grxA*, or

237 *katG* promoters essentially the same as the wild-type OxyR in the presence of H₂S_n.

238 Whereas, OxyR_{C199S}, OxyR_{C208S}, and OxyR_{C199S; C208S} all lost the regulation function

239 (Fig. 3D). Together, these results indicated that the same as in ROS sensing, only

240 Cys¹⁹⁹ and Cys²⁰⁸ are involved in H₂S_n sensing.

241 To find out the molecular mechanism on how OxyR senses H₂S_n, mass

242 spectrometry analysis was performed to analyze the H₂S_n-treated OxyR. A short

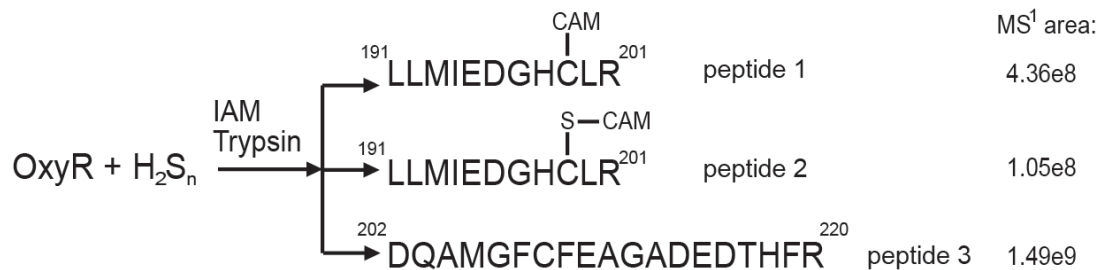
243 peptide (MW: 1356.67) containing Cys¹⁹⁹ but not Cys²⁰⁸ was identified (peptide 1, Fig.

244 7 and Fig. S2) and about 20% of it contained a persulfidation on Cys¹⁹⁹ (MW:

245 1388.64) (peptide 2, Fig. 7 and Fig. S3), according to the peak area in MS¹

246 spectrogram. A peptide containing Cys²⁰⁸ was also found, but the Cys²⁰⁸ was

247 unmodified by iodoacetamide (IAM) (MW: 2144.87) (peptide 3, Fig. 7 and Fig. S4).
248 Cys²⁰⁸ was not modified by IAM indicating that it is not accessible to IAM, consistent
249 with a previous report that Cys²⁰⁸ is buried in the protein (*Kim et al, 2002*). No
250 peptide containing both Cys¹⁹⁹ and Cys²⁰⁸ was detected. These data collectively
251 indicated that OxyR senses H₂S_n via persulfidation on Cys¹⁹⁹, other than forming
252 disulfide or -S_n- (n≥3) bond between Cys¹⁹⁹ and Cys²⁰⁸.
253



254
255 **Fig. 7. LTQ-Orbitrap tandem mass analysis of H₂S_n-reacted OxyR.** MS data of the peptides are
256 provided in Fig. S2~4.

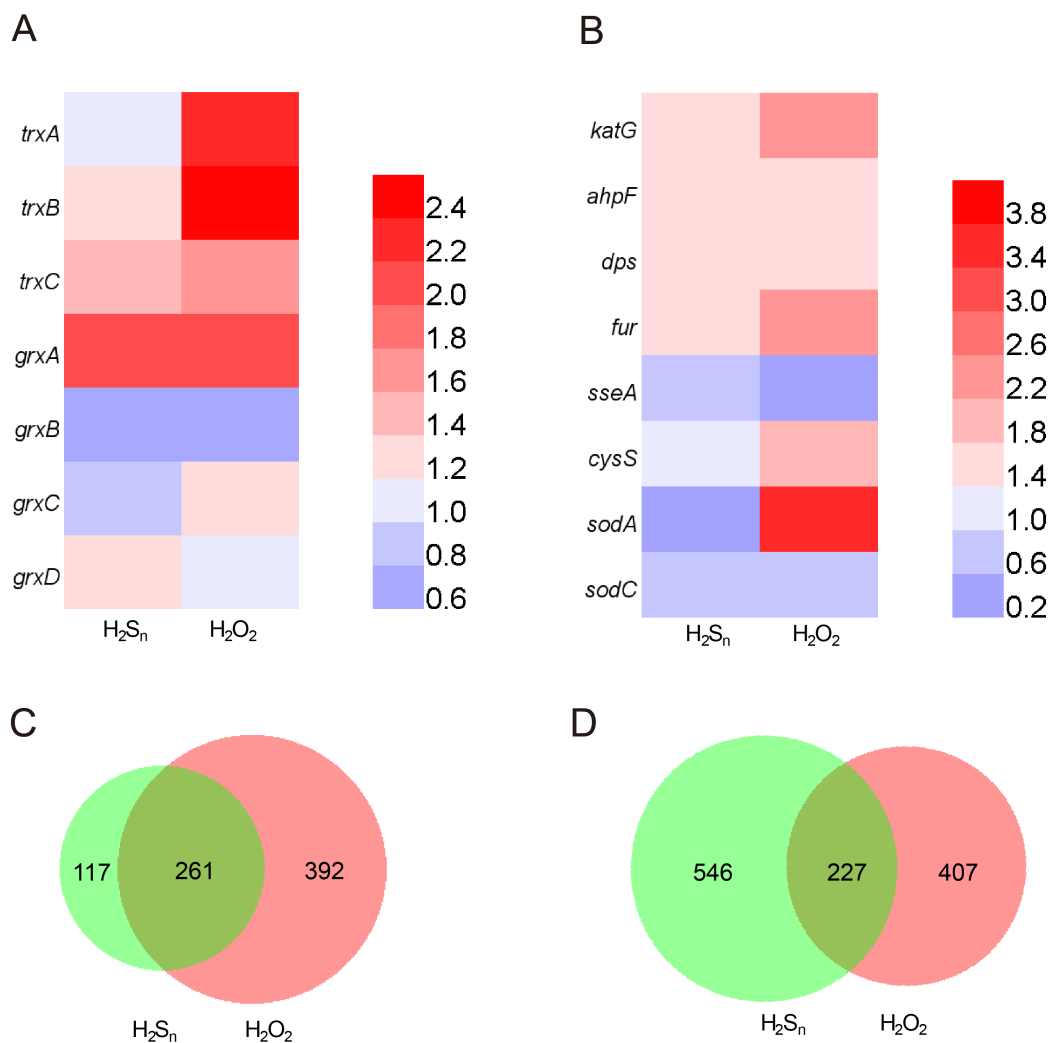
257

258 *Global transcriptome analysis of H₂S_n-stressed and H₂O₂-stressed E. coli.*

259 To systematic understand the effect of H₂S_n on *E. coli* and any similarities with
260 the H₂O₂ stress, we analyzed transcriptome response of *E. coli* with or without H₂S_n
261 stress. In the presence of 400 μM H₂S_n, *E. coli* significantly downregulated its energy
262 metabolism-related genes, such as maltoporin (71.3 fold-change) and
263 glycerol-3-phosphate transporter (33.7 fold-change). The most up regulated genes
264 included phage holin (425.9 fold-change), phage recombination protein Bet (96
265 fold-change), and a putative single-stranded DNA binding protein, suggesting that
266 H₂S_n is toxic to *E. coli* (*Xu et al, 2018*). When we checked sulfane sulfur-removing
267 enzymes, GrxA had the highest (2.1 fold) and TrxC and KatG had mild (1.6 fold and

268 1.5 fold) transcriptional increases in H₂S_n-stressed cells (Fig. 8A), consistent with the
 269 results of fluorescence reporting systems (Fig. 3); whereas, the other sulfane
 270 sulfur-reducing enzymes TrxA, TrxB, and GrxD had no obvious transcriptional
 271 change, and GrxB and GrxC had a slight decrease (Fig. 8A and 8B). These proteins
 272 are regulated by nutrient related regulators and are highly abundant in *E. coli* (Lim et
 273 al, 2000; Srivatsan & Wang, 2008) (Fernandes et al, 2005; Fernandes & Holmgren,
 274 2004; Ritz et al, 2000), suggesting that they may play the “house-keeping” role and
 275 the OxyR related GrxA, TrxC and KatG are in stress responses..

276



277

278 **Fig. 8. Transcriptome analysis of H₂S_n- or H₂O₂-stressed *E. coli*.** A, B) Transcriptional change of
279 genes involved in sulfane sulfur production and reduction. C) Numbers of transcriptionally upregulated
280 genes by H₂S_n and H₂O₂ stresses. D) Numbers of transcriptionally downregulated genes by H₂S_n and
281 H₂O₂ stresses.

282

283 At a global level, there were also similarities and differences. Among the 1286
284 genes affected by H₂O₂, upregulated and downregulated ones were 652 and 634,
285 respectively; whereas, among the 1150 genes affected by H₂S_n stress, only about 1/3
286 were upregulated (Fig. 8C and D). Gene ontology (GO) analysis indicated the cellular
287 processes affected by them were different. For instance, H₂S_n stress upregulated more
288 genes pertaining to cellular component, e.g., cell part (GO:0044464) and
289 macromolecular complex (GO:0032991), and downregulated more genes pertaining
290 to molecular function, such as molecular transducer activity (GO:0060089) and signal
291 transducer activity (GO:0004871); whereas H₂O₂ stress upregulated more genes
292 pertaining to molecular function, e.g., ribonucleotide binding (GO:0032553) and
293 carbohydrate derivative binding (GO:0097367), and downregulated no gene
294 pertaining to cellular component (Fig. S5 and S6). The TCA cycle is upregulated by
295 H₂S_n stress but downregulated by H₂O₂ stress; biosynthesis of secondary metabolites
296 (i.e. serine hydroxymethyltransferase, beta-galcosidase,
297 3-deoxy-7-phosphoheptulonate synthase, etc.) is downregulated by H₂S_n stress but not
298 affected by H₂O₂ stress (Fig. S7 and S8).

299 H₂S_n stress downregulated the expression of 3-MST (encoded by *sseA*), *SodA*,
300 and *SodC*, but did not affect the expression of *CARS* (encoded by *cysS*) (Fig. 8B).

301 These four enzymes are all involved in sulfane sulfur generation. Whereas, H₂O₂

302 stress significantly upregulated the expression of CARS and SodA, consistent with the
303 report that proteins involved in sulfane sulfur biosynthesis are induced under
304 oxidative stress because sulfane sulfur functions as antioxidants (*Fukuto et al, 2018*).
305 GrxA, TrxC, and KatG were similarly upregulated by H₂S_n and H₂O₂ stress; Trx A
306 and TrxB were not obviously affected by H₂S_n stress, but H₂O₂ stress upregulated
307 them (Fig. 8A and B). Overall, the transcriptomic data indicated that H₂S_n and H₂O₂
308 stresses lead to largely different responses in *E. coli*. However, some proteins like
309 TrxC, GrxA, and KatG, are likely involved in alleviating both stresses.

310

311 *The distribution of OxyR in sequenced bacterial genomes*

312 Several sulfane sulfur-sensing TFs have been discovered, and all are involved in
313 regulating the genes involved in sulfur oxidation (*H et al, 2017; Lira et al, 2018;*
314 *Luebke et al, 2014*). OxyR is the first global gene regulator that also senses sulfane
315 sulfur. Thus, we investigated the distribution of OxyR among 8286 microbial genomic
316 sequences (NCBI updated until November 11, 2017) by using BLAST search, and
317 then confirmed with the conserved domain and phylogenetic tree analysis. 4772
318 identified OxyR distributed in 4494 bacterial genomes, including 2432
319 Gammaproteobacteria, 887 Bataproteobacteria, 478 Alphaproteobacteria, 287
320 Corynebacteriales, 130 Flavobacteriia, 67 Streptomycetales, and 63 Bacterioidia; the
321 other 24 classes had few genomes containing OxyR (Table S1). Thus, OxyR is widely
322 distributed in bacteria. It is worth noting that OxyR is also present in many obligate
323 anaerobic bacteria, such as *Bacteroides* spp., *Prevotella* spp., and *Porphromonas* spp.

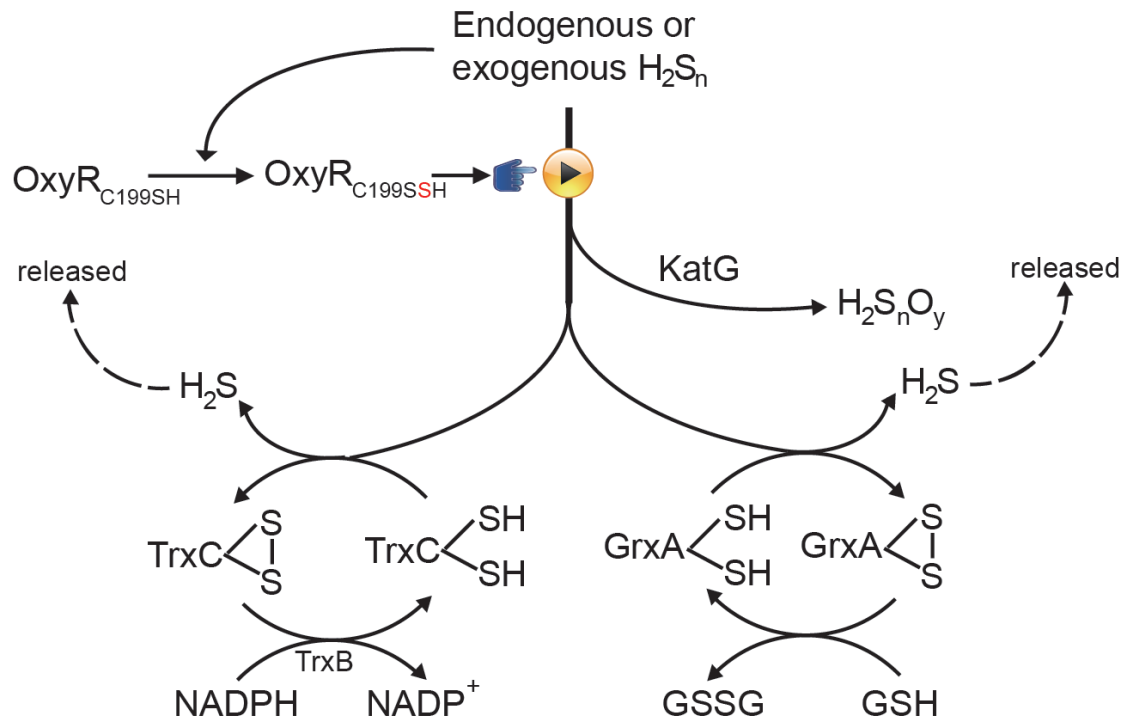
324 Some of them are common residents in the human gut. For anaerobic bacteria, OxyR
325 is more likely to deal with H₂S_n stress than H₂O₂ stress, as the latter is not an issue
326 under anaerobic conditions. It is noteworthy that intestinal tract is an anoxic and
327 sulfur rich environment (*Daeffler et al, 2017; Espey, 2013*). Hence for intestinal
328 bacteria such as *E. coli* and *Salmonella enterica*, OxyR may play important roles for
329 their survival in the gut.

330

331 **Discussion:**

332 In this study, we reported the fifth type modification of OxyR, C199-SSH, which
333 is modified by H₂S_n. H₂S_n-modified OxyR upregulates the expression of TrxC, GrxA,
334 and KatG; these enzymes can convert sulfane sulfur to releasable H₂S or H₂S_nO_y (Fig.
335 9). Other OxyR-regulated proteins like hydroperoxide reductase AhpF, DNA
336 protection protein Dps, and transcriptional regulator Fur are also upregulated under
337 H₂S_n stress (Fig. 8A). Therefore, as other modifications (*Haridas et al, 2005; Kim et*
338 *al, 2002; Seth & Stamler, 2012*), C199-SSH should also lead to multi-level
339 transcriptional responses. Although Cys²⁰⁸ is not modified by H₂S_n, it plays a critical
340 role during H₂S_n sensing, probably stabilizing the active C199-SSH.

341



342

343 **Fig. 8. Schematic representation of the OxyR-regulated RSS reduction pathways in *E. coli*.**

344

345 Reactive sulfane sulfur species are essential intracellular contents. They are
 346 beneficial at low levels (*Ida et al, 2014; Mustafa et al, 2009; Paul & Snyder, 2015*);
 347 however, they are toxic at high levels. Our systematic study of H₂S_n stress unveiled
 348 that TrxA, TrxB, GrxB, GrxC and GrxD may function as a house-keeping machinery
 349 to prevent the buildup of intracellular RRS to toxic levels; OxyR-regulated GrxA,
 350 TrxC and KatG may function as emergency backups to deal environmentally
 351 confronted or abnormally over-accumulated sulfane sulfur. Glutathione redoxins and
 352 thioredoxins reduce sulfane sulfur to H₂S that is released out of the cell for
 353 microorganisms growing under anaerobic conditions (*Abe et al, 2007; Sato et al, 2011;*
 354 *Xia et al, 2017*). For bacteria or animal host with SQR, the released H₂S is captured
 355 and oxidized back to sulfane sulfur under aerobic conditions (*Lagoutte et al, 2010*).

356 For *E. coli* and bacteria without SQR, H₂S will be released even under aerobic
357 conditions (*Li et al, 2019; Xia et al, 2017*).

358 S and O are both chalcogens. Reactive sulfane sulfur species are similar
359 chemicals to ROS (e.g., HSSH vs H₂O₂) (*Deleon et al, 2016*); their modifications to
360 proteins are also analogous, i.e., protein-SSH vs protein-SOH (*Mishanina et al, 2015*).
361 From an evolutionary perspective, the former's history can be traced back before the
362 Great Oxidation Event (GOE), when O₂ had not been generated by cyanobacteria. As
363 an abundant element on ancient earth, S should play important roles in ancient
364 microorganisms. Therefore, sulfur metabolism related enzymes had emerged before
365 the oxygen's era. It is reasonable to speculate that the anti-ROS proteins are derived
366 from anti-sulfane sulfur ones (*Olson et al, 2017*). Possibly that is the reason why the
367 anti-ROS network largely overlaps with that of anti-sulfane sulfur. On the other hand,
368 we also observed that *E. coli* has obviously responding-discrepancies when
369 confronting H₂O₂ or HSSH (Fig. 7). These discrepancies are in agreement with the
370 multi-level transcriptional responses of OxyR when activated by different reagents
371 (*Haridas et al, 2005; Kim et al, 2002; Seth & Stamler, 2012*).

372 In conclusion, we discovered that *E. coli* uses thioredoxins, glutaredoxins, and
373 catalase to control homeostasis of intracellular sulfane sulfur. OxyR functions as a
374 reactive sulfane sulfur sensor via persulfidation of its Cys¹⁹⁹ both under aerobic or
375 anoxic conditions. This is the fifth type modification observed for OxyR activation.
376 Since OxyR is widely distributed in both aerobic and anaerobic bacteria, the
377 OxyR-regulated network may represent a conserved mechanism that bacteria can

378 resort to when confronting endogenous and/or exogenous sulfane sulfur stress.

379

380 **Materials and Methods:**

381 *Strains, plasmids, and chemicals*

382 All strains and plasmids used in this study are listed in Table S2. Deletion of *oxyR*
383 was performed following a reported method (*Datsenko & Wanner, 2000*). *E. coli*
384 strains were grown in Lysogeny broth (LB) medium. Antibiotics (50 µg/ml) were
385 added when required. SSP4 (3',6'-Di(*O*-thiosalicyl)fluorecein) was purchased from
386 DOJINDO MOLECULAR TECHNOLOGIES (*Bibli et al, 2018*). H₂S_n was prepared
387 by following Kamyshny & Alexey's method (*Kamyshny et al, 2009*). Briefly, 13 mg
388 of sulfur powder and 70 mg of sodium sulfide were added to 5 ml of anoxic distilled
389 water under argon gas. The pH was adjusted to 9.3 with 6 M HCl. The obtained
390 product contained a mixture of H₂S_n, where n varies from 2 to 8 (*Olson et al, 2017*),
391 but at low concentration and neutral pH, H₂S₂ is dominant (*Bogdándi et al, 2018; Xin*
392 *et al, 2016*).

393

394 *Endogenous sulfane sulfur analysis*

395 SSP4 probe was used for batch analysis. Cells were washed with and resuspended in
396 HEPES buffer (50 mM, pH 7.4); then 10 µM SSP4 and 0.5 mM CTAB were added.
397 After an incubation at 37°C for 15 min in the dark with gently shaking (125 rpm),
398 reagents were washed off with HEPES buffer (50 mM, pH 7.4). Reacted-cells were
399 subjected to flow cytometry (FACS) analysis by using BD Accuri™ C5. For each

400 sample, >10,000 cells were analyzed in FL1-A channel. The average fluorescent
401 intensity was used.

402 The CstR-based reporting system was used for real-time analysis. *cstR* gene was
403 chemically synthesized by Genewiz (Shanghai) company and expressed with *P_{lact}*
404 promoter in pTrcHis2A plasmid, where the *trc* promoter was replaced by the CstR
405 cognate promoter, and a *mkate* gene (with a C-terminus degradation tag *ssrA*) was put
406 after it (Table S2, entry 22). For *trxA*, *trxB*, *grxB*, *grxC*, or *grxD* overexpression
407 experiment, the gene was put after *mkate*, separated by an *rbs* sequence (Table S2,
408 entries 23~27). *E. coli* strains containing reporting plasmids were culture in LB
409 medium at 37°C with shaking (220 rpm). Fluorescence was analyzed by FACS
410 (FL3-A channel, >10,000 cells).

411

412 *Hydrogen sulfide production analysis*

413 Production of hydrogen sulfide was determined using a previously reported method
414 (*Kimura et al, 2015*). Briefly, hydrogen sulfide was derivatized with mBBr then
415 analyzed by HPLC (LC-20A, Shimadzu) equipped with a fluorescence detector
416 (RF-10AXL, Shimadzu). A C18 reverse phase HPLC column (VP-ODS, 150 × 4 mm,
417 Shimadzu) was pre-equilibrated with 80% Solvent A (10% methanol and 0.25%
418 acetic acid) and 20% Solvent B (90% methanol and 0.25% acetic acid). The column
419 was eluted with the following gradients of Solvent B: 20% from 0 to 10 min; 20%–40%
420 from 10 to 25 min; 40%–90% from 25 to 30 min; 90%–100% from 30 to 32 min; 100%
421 from 32 to 35 min; 100 to 20% from 35 to 37 min; and 20% from 37 to 40 min. The

422 flow rate was 0.75 ml/min. For detection, the excitation wavelength was set to 340 nm
423 and emission wavelength was set to 450 nm.

424

425 *H₂S_n inhibition and induction tests*

426 For growth inhibition test, middle-log phased *E. coli* cells (OD₆₀₀=0.8) were diluted
427 and dripped in freshly prepared LB agar medium containing 0 or 100 μM H₂S_n and
428 incubated in 37°C under aerobic conditions. For anaerobic conditions, the anaerobic
429 LB agar plates were prepared in an anaerobic glove box and the dilution and drip of *E.*
430 *coli* cells also performed in an anaerobic glove box, then incubated in an anaerobic
431 incubator at 37°C for 24 hours. For promoter induction test, a *mkate* gene was put
432 after *trxC*, *grxA*, or *katG* native promoter in pTrchis2A plasmid (Table S2, entries
433 17~19). The *oxyR* or its mutant gene was expressed under the *P_{lacI}* promoter in the
434 same plasmid (Table S2, entries 5~16) for complementary experiments. The obtained
435 plasmids were transformed into *wt* and Δ *oxyR* strains. Early log-phased *E. coli* cells
436 (OD₆₀₀= 0.5, in liquid LB) were incubated with 600 μM H₂S_n for 2 hours. Cells were
437 harvested and washed with HEPES buffer (50 mM, pH 7.4), then subjected to FACS
438 analysis (FL3-A channel, >10,000 cells).

439

440 *Real-time quantitative reverse transcription PCR (RT-qPCR)*

441 RNA sample was prepared by using the TRIzol™ RNA Purification Kit (12183555,
442 Invitrogen). Total cDNA was synthesized using the All-In-One RT Master Mix
443 (ABM). For RT-qPCR, strains were grown in anaerobic LB medium until OD₆₀₀

444 reached 0.4, and then 200 μM H_2S_n were added into anaerobic bottle. After 60 min,
445 cells were collected by centrifugation and RNA was extracted. RT-qPCR was
446 performed by using the Bestar SybrGreen qPCR Mastermix (DBI) and LightCycler
447 480II (Roche). For calculation the relative expression levels of tested genes, GAPDH
448 gene expression was used as the internal standard.

449

450 *Protein purification and reaction with DTT or H_2S_n*

451 The *oxyR* gene with a C-terminal His tag was ligated into pET30. Mutants of *oxyR*
452 were constructed from this plasmid via site-directed mutagenesis (*Xia et al, 2015*).
453 The obtained plasmids were transformed into *E. coli* BL21 (DE3). For protein
454 expression, *E. coli* cells were cultured in LB medium at 25°C with shaking (150 rpm)
455 until OD_{600} reacted 0.6–0.8, 0.4 mM isopropyl- β -D-thiogalactopyranoside (IPTG)
456 was added, and cells were cultured for additional 16 hours at 16°C. Cells were then
457 harvested and disrupted through a high pressure cracker SOCH-18 (STANSTED);
458 protein was purified via the Ni-NTA resin (Invitrogen). Buffer exchange of the
459 purified protein was performed by using PD-10 desalting column (GE Healthcare).

460 Reactions were performed in an anaerobic glove box. 0.6 mg/ml protein was
461 mixed with 200 mM DTT in a pH 8.0 buffer (50 mM NaH_2PO_4 , 300 mM NaCl). After
462 1-hour incubation at RT, the protein was dialyzed against 0.5 M KCl until the dialysis
463 buffer was free of DTNB-titratable SH group. For H_2S_n reaction, the reduced OxyR
464 was mixed with about 10-fold concentration of H_2S_n and incubated for 30 min at RT.
465 Unreacted H_2S_n was removed via dialysis. The reacted-proteins were sealed and taken

466 out from the glove box to be used in further experiments.

467

468 *LC-MS/MS analysis of OxyR*

469 The H₂S_n-reacted OxyR (0.5 mg/ml) was mixed with iodoacetamide (IAM), and
470 then digested with trypsin by following a previously reported protocol (*H et al, 2017*).

471 The Prominence nano-LC system (Shimadzu) equipped with a custom-made silica
472 column (75 μm × 15 cm) packed with 3-μm Reprosil-Pur 120 C18-AQ was used for

473 the analysis. For the elution process, a 100 min gradient from 0% to 100% of solvent

474 B (0.1 % formic acid in 98% acetonitrile) at 300 nl/min was used; solvent A was 0.1 %

475 formic acid in 2% acetonitrile. The eluent was ionized and electrosprayed via

476 LTQ-Orbitrap Velos Pro CID mass spectrometer (Thermo Scientific), which run in

477 data-dependent acquisition mode with Xcalibur 2.2.0 software (Thermo Scientific).

478 Full-scan MS spectra (from 400 to 1800 m/z) were detected in the Orbitrap with a

479 resolution of 60,000 at 400 m/z.

480

481 *In vitro transcription-translation analysis*

482 *In vitro* translation-transcription reactions were performed using the Purepress *In*

483 *Vitro* Protein Synthesis system (NEB #E6800). The reaction solution was prepared in

484 the following order: 10 μL solution A (NEB #E6800), 7.5 μL solution B (NEB

485 #E6800), 2 μL *E. coli* RNA polymerase (NEB #M0551), 1 μL RNase inhibitor, 500

486 ng DTT- or H₂S_n- reacted protein, 200 ng DNA fragment containing P_{TrxC}-mKate, and

487 RNase free water. The total volume was 25 μL. The solution was incubated at 37°C

488 for 3 hours. After reaction, the translated mKate was diluted four times with distilled
489 water, and assayed by using the Synergy H1 microplate reader. The excitation
490 wavelength was set to 588 nm, and the emission wavelength was set to 633 nm. The
491 fluorescence intensity from reduced OxyR was used as standard; fluorescence
492 intensities from other groups were divided by the standard to calculate the relative
493 expression levels.

494

495 *Transcriptomic analysis*

496 *E. coli wt* strain was cultured in LB medium until OD₆₀₀ reached 0.5, and 500 μM
497 H₂S_n or 500 μM H₂O₂ were added. After 20 min of treatment, cells were harvested
498 and total RNA was extracted by using the TRIzolTM RNA Purification Kit (12183555,
499 Invitrogen). RNA quality was assessed with the RNA Nano 6000 Assay Kit of the
500 Agilent Bioanalyzer 2100 system (Agilent Technologies). rRNA was removed with
501 the Ribo-Zero rRNA Removal Kit (MRZMB 126, Epicentre Biotechnologies). For
502 cDNA library construction, first-strand cDNA was synthesized by using random
503 hexamer primers from fragmentation of mRNA and second-strand cDNA was
504 synthesized by using a dNTP mixture containing dUTP with DNA polymerase I and
505 RNase H. After adenylation of the ends of blunt-ended DNA fragments, NEBNext
506 index adaptor oligonucleotides were ligated to the cDNA fragments. The
507 second-strand cDNA containing dUTP was digested with the USER enzyme. The
508 first-strand DNA fragments with ligated adaptors on both ends were selectively
509 enriched in a 10-cycle PCR reaction, purified (AMPure XP), and the library was

510 quantified using the Agilent High Sensitivity DNA assay on the Agilent Bioanalyzer
511 2100 system. The library was sequencing on Illumina Hiseq 2500 platform.
512 Sequencing was performed at Beijing Novogene Bioinformatics Technology Co., Ltd.
513 The clean data were obtained from raw data by removing reads containing adapter,
514 poly-N and low quality reads. The clean reads were aligned with the genome of *E.*
515 *coli* BL21 by using Bowtie2-2.2.3. Gene expression was quantified as reads per
516 kilobase of coding sequence per million reads (RPKM) algorithm. Genes with a
517 p-value<0.05 found by DESeq and change fold>1.5 were considered as significantly
518 differentially expressed. Gene Ontology (GO) and KEGG analyses were performed at
519 NovoMagic platform provided by Beijing Novogene Bioinformatics Technology Co.,
520 Ltd.
521
522 *Analysis of OxyR distribution in sequenced bacterial genomes.*
523 A microbial genomic protein sequence set from NCBI updated until November 11,
524 2017 was downloaded for OxyR search. The query sequences of OxyR were reported
525 OxyR proteins (*Choi et al, 2001; Inseong et al, 2015; Kaewkanya et al, 2003*) and
526 were used to search the database by using Srandalone BLASTP algorithm with
527 conventional criteria (e-value $\leq 1e^{-5}$, coverage $\geq 45\%$, identity $\geq 30\%$) to obtain
528 OxyR candidates from 8286 bacterial genomes. A conserved domain PBP2_OxyR
529 and PRK11151 were used as standard features for further filtration of OxyR
530 candidates. The candidates containing PBP2_OxyR or PRK11151 were identified as
531 putative OxyR.

532

533 **Acknowledgments**

534 The work was financially supported by grants from the National Natural Science

535 Foundation of China (91751207, 31770093), the National Key Research and

536 Development Program of China (2016YFA0601103), and the Natural Science

537 Foundation of Shandong Province (ZR2016CM03, ZR2017ZB0210).

538

539 **References**

540 Abe K, Kimura H. 1996. The possible role of hydrogen sulfide as an endogenous
541 neuromodulator. *J Neuroscience* **16**: 1066-1071.

542

543 Abe T, Hoshino T, Nakamura A, Takaya N. 2007. Anaerobic elemental sulfur
544 reduction by fungus *Fusarium oxysporum*. *Journal of the Agricultural Chemical*
545 *Society of Japan* **71**: 2402-2407.

546

547 Akaike T, Ida T, Wei F-Y, Nishida M, Kumagai Y, Alam MM, Ihara H, Sawa T,
548 Matsunaga T, Kasamatsu S, Nishimura A, Morita M, Tomizawa K, Nishimura A,
549 Watanabe S, Inaba K, Shima H, Tanuma N, Jung M, Fujii S et al. 2017.
550 Cysteinyl-tRNA synthetase governs cysteine polysulfidation and mitochondrial
551 bioenergetics. *Nature Communications* **8**: 1177. doi: 10.1038/s41467-017-01311-y

552

553 Bibli S-I, Luck B, Zukunft S, Wittig J, Chen W, Xian M, Papapetropoulos A, Hu J,

554 Fleming I. 2018. A selective and sensitive method for quantification of endogenous
555 polysulfide production in biological samples. *Redox Biology* **18**: 295-304.
556 <https://doi.org/10.1016/j.redox.2018.07.016>

557

558 Bogdándi V, Ida T, Sutton TR, Bianco C, Ditrói T, Koster G, Henthorn HA, Minnion
559 M, Toscano JP, Van dVA. 2019. Speciation of reactive sulfur species and their
560 reactions with alkylating agents: do we have any clue about what is present inside the
561 cell? *Br J Pharmacol* **176**:646-670. doi: 10.1111/bph.14394.

562

563 Cai WJ, Wang ML, Wang C, Zhu YC. 2010. Hydrogen sulfide induces human colon
564 cancer cell proliferation: role of Akt, ERK and p21. *Cell Biol Int* **34**: 565-572.

565

566 Carbonero F, Benefiel AC, Alizadeh-Ghamsari AH, Gaskins HR. 2012. Microbial
567 pathways in colonic sulfur metabolism and links with health and disease. *Frontiers in*
568 *Physiology* **3**: 448. doi: 10.3389/fphys.2012.00448.

569

570 Choi H-J, Kim S-J, Mukhopadhyay P, Cho S, Woo J-R, Storz G, Ryu S-E. 2001.
571 Structural basis of the redox switch in the OxyR transcription factor. *Cell* **105**:
572 103-113. [https://doi.org/10.1016/S0092-8674\(01\)00300-2](https://doi.org/10.1016/S0092-8674(01)00300-2)

573

574 Christman MF, Morgan RW, Jacobson FS, Ames BN. 1985. Positive control of a
575 regulon for defenses against oxidative stress and some heat-shock proteins in

576 *Salmonella typhimurium*. *Cell* **41**: 753-762.

577

578 Dóka É, Pader I, Bíró A, Johansson K, Cheng Q, Ballagó K, Prigge JR, Pastor-Flores

579 D, Dick TP, Schmidt EE. 2016. A novel persulfide detection method reveals protein

580 persulfide-and polysulfide-reducing functions of thioredoxin and glutathione systems.

581 *Science advances* **2**: e1500968. doi: 10.1126/sciadv.1500968.

582

583 Daeffler KNM, Galley JD, Sheth RU, Ortiz-Velez LC, Bibb CO, Shroyer NF,

584 Britton RA, Tabor JJ. 2017. Engineering bacterial thiosulfate and tetrathionate sensors

585 for detecting gut inflammation. *Molecular Systems Biology* **13**:923. doi:

586 *10.15252/msb.20167416*.

587

588 Datsenko KA, Wanner BL. 2000. One-step inactivation of chromosomal genes in

589 *Escherichia coli* K-12 using PCR products. *Proceedings of the National Academy of*

590 *Sciences of the United States of America* **97**: 6640-6645.

591

592 Deleon ER, Gao Y, Huang E, Arif M, Arora N, Divietro A, Patel S, Olson KR. 2016.

593 A case of mistaken identity: are reactive oxygen species actually reactive sulfide

594 species? *Am J Physiol Regul Integr Comp Physiol* **310**: R549.

595

596 Espey MG. 2013. Role of oxygen gradients in shaping redox relationships between

597 the human intestine and its microbiota. *Free Radical Biology & Medicine* **55**:

598 130-140.

599

600 Fernandes AP, Fladvad M, Berndt C, Andrésen C, Lillig CH, Neubauer P,
601 Sunnerhagen M, Holmgren A, Vlamis-Gardikas A. 2005. A novel monothiol
602 glutaredoxin (Grx4) from *Escherichia coli* can serve as a substrate for thioredoxin
603 reductase. *J Biol Chem* **280**: 24544-24552.

604

605 Fernandes AP, Holmgren A. 2004. Glutaredoxins: glutathione-dependent redox
606 enzymes with functions far beyond a simple thioredoxin backup system. *Antioxid*
607 *Redox Signal* **6**: 63-74.

608

609 Fujii S, Sawa T, Motohashi H, Akaike T. 2019. Persulfide synthases that are
610 functionally coupled with translation mediate sulfur respiration in mammalian cells.
611 *Br J Pharmacol* **176**:607-615. doi: 10.1111/bph.14356.

612

613 Fukuto JM, Ignarro LJ, Nagy P, Wink DA, Kevil CG, Feelisch M, Cortese-Krott MM,
614 Bianco CL, Kumagai Y, Hobbs AJ, Lin J, Ida T, Akaike T. 2018. Biological
615 hydropersulfides and related polysulfides – a new concept and perspective in redox
616 biology. *FEBS Lett* **592**: 2140-2152. doi:10.1002/1873-3468.13090

617

618 Gao XH, Krokowski D, Guan BJ, Bederman I, Majumder M, Parisien M, Diatchenko
619 L, Kabil O, Willard B, Banerjee R. 2015. Quantitative H₂S-mediated protein

620 sulfhydration reveals metabolic reprogramming during the integrated stress response.

621 *Elife* **4**:e10067. doi: 10.7554/eLife.10067.

622

623 Gutierrez-Ríos RM, Freyre-Gonzalez JA, Resendis O, Collado-Vides J, Saier M,

624 Gosset G. 2007. Identification of regulatory network topological units coordinating

625 the genome-wide transcriptional response to glucose in *Escherichia coli*. *BMC*

626 *Microbiol* **7**: 53-53.

627

628 Li H, Li J, Lü C, Xia Y, Xin Y, Liu H, Xun L, Liu H. 2017. FisR activates

629 $\sigma(54)$ -dependent transcription of sulfide-oxidizing genes in *Cupriavidus*

630 *pinatubonensis* JMP134. *Mol Microbiol* **105**: 373-384. doi: 10.1111/mmi.13725.

631

632 Haridas V, Kim SO, Nishimura G, Hausladen A, Stamler JS, Gutterman JU. 2005.

633 Avicinylation (thioesterification): a protein modification that can regulate the

634 response to oxidative and nitrosative stress. *Proceedings of the National Academy of*

635 *Sciences of the United States of America* **102**: 10088-10093.

636

637 Hine C, Harputlugil E, Zhang Y, Ruckstuhl C, Lee BC, Brace L, Longchamp A,

638 Treviño-Villarreal J, Mejia P, Ozaki CK. 2015. Endogenous hydrogen sulfide

639 production is essential for dietary restriction benefits. *Cell* **160**: 132-144.

640

641 Ida T, Sawa T, Ihara H, Tsuchiya Y, Watanabe Y, Kumagai Y, Suematsu M,

642 Motohashi H, Fujii S, Matsunaga T. 2014. Reactive cysteine persulfides and
643 S-polythiolation regulate oxidative stress and redox signaling. *Proceedings of the*
644 *National Academy of Sciences* **111**: 7606-7611.

645

646 Inseong J, In-Young C, Hee-Won B, Jin-Sik K, Saemee S, You-Hee C, Nam-Chul H.
647 2015. Structural details of the OxyR peroxide-sensing mechanism. *Proceedings of the*
648 *National Academy of Sciences of the United States of America* **112**: 6443-6448.

649

650 Islamov RA, Bishimova I, Sabitov AN, Ilin AI, Burkitbaev MM. 2018. Lack of
651 mutagenic activity of sulfur nanoparticles in micronucleus test on L5178Y Cell
652 Culture. *Cell & Tissue Biology* **12**: 27-32.

653

654 Kaewkanya N, Skorn M, Paiboon V. 2003. The OxyR from *Agrobacterium*
655 *tumefaciens*: evaluation of its role in the regulation of catalase and peroxide responses.
656 *Biochemical & Biophysical Research Communications* **304**: 41-47.

657

658 Kamyshny A, Borkenstein CG, Ferdelman TG. 2009. Protocol for quantitative
659 detection of elemental sulfur and polysulfide zero-valent sulfur distribution in natural
660 aquatic samples. *Geostandards and Geoanalytical Research* **33**: 415-435.
661 10.1111/j.1751-908X.2009.00907.x

662

663 Kim SO, Merchant K, Nudelman R, Jr WFB, Keng T, Deangelo J, Hausladen A,

- 664 Stamler JS. 2002. OxyR : A Molecular Code for Redox-Related Signaling. *Cell* **109**:
665 383-396.
- 666
- 667 Kimura Y, Toyofuku Y, Koike S, Shibuya N, Nagahara N, Lefer D, Ogasawara Y,
668 Kimura H. 2015. Identification of H₂S₃ and H₂S produced by 3-mercaptopyruvate
669 sulfurtransferase in the brain. *Scientific Reports* **5**: 14774. 10.1038/srep14774
670 <https://www.nature.com/articles/srep14774#supplementary-information>
- 671
- 672 Lagoutte E, Mimoun S, Andriamihaja M, Chaumontet C, Blachier F, Bouillaud F.
673 2010. Oxidation of hydrogen sulfide remains a priority in mammalian cells and causes
674 reverse electron transfer in colonocytes. *Biochim Biophys Acta* **1797**: 1500-1511.
- 675
- 676 Li K, Xin Y, Xuan G, Zhao R, Liu H, Xia Y, Xun L. 2019. *Escherichia coli* uses
677 different enzymes to produce H₂S and reactive sulfane sulfur from L-cysteine.
678 *Frontiers in Microbiology* **10**: 298. doi: 10.3389/fmicb.2019.00298
- 679
- 680 Lim CJ, Daws T, Gerami-Nejad M, Fuchs JA. 2000. Growth-phase regulation of the
681 *Escherichia coli* thioredoxin gene. *Biochim Biophys Acta* **1491**: 1-6.
- 682
- 683 Lira NPVD, Pauletti BA, Marques AC, Perez CA, Caserta R, Souza AAD, Vercesi
684 AE, Leme AFP, Benedetti CE. 2018. BigR is a sulfide sensor that regulates a sulfur
685 transferase/dioxygenase required for aerobic respiration of plant bacteria under sulfide

686 stress. *Scientific Reports* **8**:3508. doi: 10.1038/s41598-018-21974-x.

687

688 Lisjak M, Srivastava N, Teklic T, Civale L, Lewandowski K, Wilson I, Wood ME,
689 Whiteman M, Hancock JT. 2010. A novel hydrogen sulfide donor causes stomatal
690 opening and reduces nitric oxide accumulation. *Plant Physiol Biochem* **48**: 931-935.

691

692 Luebke JL, Shen J, Bruce KE, Kehl-Fie TE, Peng H, Skaar EP, Giedroc DP. 2014.
693 The CsoR-like sulfurtransferase repressor (CstR) is a persulfide sensor in
694 *Staphylococcus aureus*. *Mol Microbiol* **94**: 1343-1360. doi: 10.1111/mmi.12835

695

696 Mishanina TV, Libiad M, Banerjee R. 2015. Biogenesis of reactive sulfur species for
697 signaling by hydrogen sulfide oxidation pathways. *Nat Chem Biol* **11**: 457-464. doi:
698 10.1038/nchembio.1834

699

700 Mustafa AK, Gadalla MM, Sen N, Kim S, Mu W, Gazi SK, Barrow RK, Yang G,
701 Wang R, Snyder SH. 2009. H₂S signals through protein S-sulfhydration. *Science*
702 *signaling* **2**: ra72.

703

704 Nagahara N, Koike S, Nirasawa T, Kimura H, Ogasawara Y. 2018. Alternative
705 pathway of H₂S and polysulfides production from sulfurated catalytic-cysteine of
706 reaction intermediates of 3-mercaptopyruvate sulfurtransferase. *Biochem Biophys Res*
707 *Commun* **496**: 648-653. <https://doi.org/10.1016/j.bbrc.2018.01.056>

708

709 Olson KR, Gao Y, Arif F, Arora K, Patel S, DeLeon ER, Sutton TR, Feelisch M,
710 Cortesekrott MM, Straub KD. 2018. Metabolism of hydrogen sulfide (H₂S) and
711 production of reactive sulfur species (RSS) by superoxide dismutase. *Redox Biology*
712 **15**: 74-85.

713

714 Olson KR, Gao Y, DeLeon ER, Arif M, Arif F, Arora N, Straub KD. 2017. Catalase
715 as a sulfide-sulfur oxido-reductase: an ancient (and modern?) regulator of reactive
716 sulfur species (RSS). *Redox Biology* **12**: 325-339.
717 <https://doi.org/10.1016/j.redox.2017.02.021>

718

719 Ono K, Akaike T, Sawa T, Kumagai Y, Wink DA, Tantillo DJ, Hobbs AJ, Nagy P,
720 Xian M, Lin J. 2014. The redox chemistry and chemical biology of H₂S,
721 hydropersulfides and derived species: implications to their possible biological activity
722 and utility. *Free Radical Biology & Medicine* **77**: 82-94.

723

724 Park CM, Weerasinghe L, Day JJ, Fukuto JM, Ming X. 2015. Persulfides: current
725 knowledge and challenges in chemistry and chemical biology. *Molecular Biosystems*
726 **11**: 1775-1785.

727

728 Paul BD, Snyder SH (2015) Chapter Five - Protein Sulfhydration. In *Methods in*
729 *Enzymology*, Cadenas E, Packer L (eds), Vol. 555, pp 79-90. Academic Press

730

731 Peng H, Zhang Y, Palmer LD, Kehl-Fie TE, Skaar EP, Trinidad JC, Giedroc DP.
732 2017. Hydrogen sulfide and reactive sulfur species impact proteome S-sulfhydrylation
733 and global virulence regulation in *Staphylococcus aureus*. *ACS Infectious Diseases* **3**:
734 744-755. doi: 10.1021/acsinfecdis.7b00090

735

736 Rai M, Ingle AP, Paralikar P. 2016. Sulfur and sulfur nanoparticles as potential
737 antimicrobials: from traditional medicine to nanomedicine. *Expert review of*
738 *anti-infective therapy* **14**: 969-978. doi: 10.1080/14787210.2016.1221340.

739

740 Ritz D, Patel H, Doan B, Zheng M, Aslund F, Storz G, Beckwith J. 2000. Thioredoxin
741 2 is involved in the oxidative stress response in *Escherichia coli*. *J Biol Chem* **275**:
742 2505-2512.

743

744 Samrat RC, Amrita M, Mahua G, Sulagna B, Dipankar C, Arunava G. 2013.
745 Investigation of antimicrobial physiology of orthorhombic and monoclinic
746 nanoallotropes of sulfur at the interface of transcriptome and metabolome. *Applied*
747 *Microbiology & Biotechnology* **97**: 5965-5978.

748

749 Sato I, Shimatani K, Fujita K, Abe T, Shimizu M, Fujii T, Hoshino T, Takaya N.
750 2011. Glutathione reductase/glutathione is responsible for cytotoxic elemental sulfur
751 tolerance via polysulfide shuttle in fungi. *J Biol Chem* **286**: 20283-20291. doi:

752 10.1074/jbc.M111.225979.

753

754 Sawa T, Ono K, Tsutsuki H, Zhang T, Ida T, Nishida M, Akaike T (2018) Chapter
755 One - Reactive cysteine persulphides: occurrence, biosynthesis, antioxidant activity,
756 methodologies, and bacterial persulphide signalling. In *Advances in Microbial*
757 *Physiology*, Poole RK (ed), Vol. 72, pp 1-28. Academic Press

758

759 Seth D, Stamler JS. 2012. Endogenous protein S-Nitrosylation in *E. coli*: regulation
760 by OxyR. *Science* **336**: 470-473.

761

762 Srivatsan A, Wang JD. 2008. Control of bacterial transcription, translation and
763 replication by (p)ppGpp. *Curr Opin Microbiol* **11**: 100-105.

764

765 Storz G, Tartaglia LA, Ames BN. 1990. Transcriptional regulator of oxidative
766 stress-inducible genes: direct activation by oxidation. *Science* **248**: 189-194.

767

768 Toohey JI. 2011. Sulfur signaling: is the agent sulfide or sulfane? *Anal Biochem* **413**:
769 1-7.

770

771 Wedmann R, Onderka C, Wei S, Szijártó IA, Miljkovic JL, Mitrovic A, Lange M,
772 Savitsky S, Yadav PK, Torregrossa R. 2016. Improved tag-switch method reveals that
773 thioredoxin acts as depersulfidase and controls the intracellular levels of protein

774 persulfidation. *Chemical Science* **7**: 3414-3426.

775

776 Williams JS, Cooper RM. 2010. The oldest fungicide and newest phytoalexins – a
777 reappraisal of the fungitoxicity of elemental S. *Plant Pathol* **53**: 263-279.

778

779 Xia Y, Chu W, Qi Q, Xun L. 2015. New insights into the QuikChange™ process
780 guide the use of Phusion DNA polymerase for site-directed mutagenesis. *Nucleic
781 Acids Res* **43**: e12. doi: 10.1093/nar/gku1189.

782

783 Xia Y, Lü C, Hou N, Xin Y, Liu J, Liu H, Xun L. 2017. Sulfide production and
784 oxidation by heterotrophic bacteria under aerobic conditions. *ISME Journal* **11**: 2754
785 -2766. doi: 10.1038/ismej.2017.125.

786

787 Xin Y, Liu H, Cui F, Liu H, Xun L. 2016. Recombinant *Escherichia coli* with sulfide:
788 quinone oxidoreductase and persulfide dioxygenase rapidly oxidises sulfide to sulfite
789 and thiosulfate via a new pathway. *Environ Microbiol* **18**: 5123-5136.

790

791 Xu Z, Qiu Z, Liu Q, Huang Y, Li D, Shen X, Fan K, Xi J, Gu Y, Tang Y, Jiang J, Xu
792 J, He J, Gao X, Liu Y, Koo H, Yan X, Gao L. 2018. Converting organosulfur
793 compounds to inorganic polysulfides against resistant bacterial infections. *Nature
794 Communications* **9**: 3713. doi: 10.1038/s41467-018-06164-7

795

796 Yadav PK, Martinov M, Vitvitsky V, Seravalli J, Wedmann R, Filipovic MR,

797 Banerjee R. 2016. Biosynthesis and reactivity of cysteine persulfides in signaling. *J*

798 *Am Chem Soc* **138**: 289-99. doi: 10.1021/jacs.5b10494.

799

800 Zheng M, Åslund F, Storz G. 1998. Activation of the OxyR transcription factor by

801 reversible disulfide bond formation. *Science* **279**: 1718-1722. doi:

802 10.1126/science.279.5357.1718

803

804